http://dx.doi.org/10.5012/bkcs.2012.33.12.3993

Supercapacitive Properties of Co-Ni Mixed Oxide Electrode Adopting the Nickel Foam as a Current Collector

Hyeon Woo Cho,[†] Ji Hyun Nam,[†] Jeong Ho Park,[†] Kwang Man Kim,[‡,*] and Jang Myoun Ko[†,*]

[†]*Department of Applied Chemistry and Biotechnology, Hanbat National University, Daejeon 305-719, Korea*
[*]*E-mail: jmko@hanbat.ac.kr*
[‡]*Research Team of Power Control Devices, Electronics and Telecommunication Research Institute, Daejeon 305-700, Korea*
[*]*E-mail: kwang@etri.re.kr*
Received August 27, 2012, Accepted September 7, 2012

Three-dimensional porous nickel foam was used as a current collector to prepare a Co-Ni oxide/Ni foam electrode for a supercapacitor. The synthesized Co-Ni oxide was proven to consist of mixed oxide phases of Co_3O_4 and NiO. The Co-Ni oxide/Ni foam electrode prepared was characterized by morphological observation, crystalline property analysis, cyclic voltammetry, and impedance spectroscopy. Cyclic voltammetry for the electrode showed high specific capacitances, such as 936 F g^{-1} at 5 mV s^{-1} and 566 F g^{-1} at 200 mV s^{-1}, and a comparatively good cycle performance. These improved results were mainly due to the dimensional stability of the nickel foam and its high electrical contact between the electrode material and the current collector substrate.

Key Words : Cobalt-nickel oxide, Nickel foam current collector, Supercapacitor, Cyclic voltammetry

Introduction

Recent progress in portable electronics, hybrid electric vehicles, and power backup modules has greatly increased the demands for high power energy devices for limited time intervals. Supercapacitor is one of very promising energy devices that would satisfy these types of requirements due to their ultrahigh power performance with high capacitance and excellent cycle performance. There is also an advantage of being able to store a greater amount of energy because contributions by both the electric double layer formed on the electrode surfaces and by the faradaic redox reaction can be attributed to the capacitance increase in a supercapacitor. Carbonaceous compounds, metal oxides, and conducting polymers have been studied intensively and extensively as active materials for the construction of supercapacitive electrodes with high surface area. Carbonaceous materials, including active carbon, carbon nanotubes, carbon nanofibers, or carbon aerogels, showed a maximum capacitance of about 250 F g^{-1}, but exhibited comparatively low specific energy density.[1] Conducting polymers with a higher redox activity, including polypyrrole, polyaniline, or polythiophene, demonstrated a wide range of specific capacitances (100-800 F g^{-1}) but showed weak mechanical strength and poor cycle performance.[2,3] In contrast, metal oxides such as RuO_2, IrO_2, and MnO_2 were shown to exhibit superior capacitance, *e.g.*, higher than 1000 F g^{-1} for RuO_2.[4,5] However, there were some drawbacks, such as the limited utilization of the thin surface layer of bulk RuO_2, low rate-capability, and expensive cost of materials. Many studies to overcome such drawbacks of RuO_2 have been tried: the use of hydrous RuO_2 or its hydrates[6,7] resulting in higher rate-capability, and improved utilization of RuO_2 by adopting nm-sized substrates.[8]

Nickel oxide,[9-13] cobalt oxide,[14-19] and Co-Ni mixed oxide[20,21] have been studied as alternative electrode materials to RuO_2. Nickel oxide was seen as a possibility to improve the capacitance and to enhance charge-storage capability by the control of surface morphology.[11] Cobalt oxide is known as a superior supercapacitor electrode material due to its high efficiency, long cycle life, and excellent resistance to corrosion.[18,19] Hu and Cheng[21] demonstrated that binary hydrous Co-Ni oxide showed a large capacitance of *ca.* 730 F g^{-1} at 25 mV s^{-1} and 4 °C, due to its highly porous nature. The benefit, obtainable by simultaneous use of Co and Ni oxides, was originated from the fact that the electrochemical reversibility could be improved by the introduction of cobalt ions into the nickel oxide matrix in the nickel-metal hydride battery.[22]

On the other hand, the electrochemical properties, in particular the specific capacitance, can be very much influenced by the use of a nickel form as a current collector in a supercapacitor electrode. For instance, porous nickel foam has many useful features including enhancing the dimensional stability of an electrode, increasing the electrical conductivity, and decreasing the contact resistance between current collector and the active material. Three-dimensional porous nickel foam has been used as a current collector in the nickel-metal hydride battery[23,24] and also in the active carbon-based supercapacitor, and it shows a higher capacitance than in the case of using nickel foil current collector.[25] The use of a nickel foam substrate can be expected to exhibit performance improvement in a cobalt oxide electrode of a supercapacitor adopting the nickel foam as a current collector, which is providing another electrochemical active site.

Combining such dual concepts described above, we prepare in this paper a Co-Ni mixed oxide electrode on the nickel foam current collector to obtain a superior supercapacitor showing much higher capacitance with stable

cycleability. We also discuss the effect of adopting the nickel foam on the charge accumulation behavior and cycling stability by the surface morphology observation, crystalline phase analysis, and the investigation of electrochemical supercapacitive properties.

Experimental

The nickel foam used was a three-dimensional porous network (Shenzhen Rolinsia Power Materials Ltd.) with a thickness of 1.0 mm and a porosity of 110 pores per inch. The surface image of the nickel foam can be examined by scanning electron microscopy, as shown in Figure 1(a). Prior to use, the nickel foam was pressed to 0.6 mm, washed with acetone (2-3 times) and distilled water (2-3 times), and dried at ambient temperature. The pristine Ni foam (1 cm × 1 cm, approximately 0.05 g) was at first characterized by the cyclic voltammetry (CV) under the same conditions to the Co-Ni mixed oxide case, which would be described below in detail. Starting material for the Co-Ni mixed oxide was an aqueous mixture consisting of 1 M $Co(NO_3)_2 \cdot 6H_2O$ (Aldrich) and 1 M $Ni(NO_3)_2 \cdot 6H_2O$ (Aldrich). The Co-Ni oxide electrode was prepared by coating the nickel foam with the mixture without any binder material, drying at room temperature for 24 h, and annealing at 250 °C for 2 h. The surface image of the synthesized Co-Ni oxide electrode was observed using a scanning electron microscope (JSM-6300, Jeol) equipped with an energy dispersive spectroscope. The crystalline phases of the Co-Ni oxide powder, which had already been sampled from the Co-Ni oxide/Ni foam electrode, were also investigated using an X-ray diffractometer (Rigaku) in the Bragg angle range of 10-80°.

A CV test was performed to investigate the supercapacitive properties using a potentiostat/galvanostat (P/Gstat-100, Autolab) equipped with a capillary reference electrode, keeping a distance of 1-2 mm between the capillary and the working electrode (Co-Ni oxide/Ni foam, 1 cm × 1 cm) to minimize the voltage (*iR*) drop in the electrolyte solution. The reference and counter electrodes used were a Ag/AgCl (3 M KCl, 0.196 V *vs* SCE, Metrohm) and a platinum foil (2 cm × 2 cm), respectively. An aqueous solution of 1 M KOH, purged by nitrogen gas for 1 h to evacuate the dissolved oxygen component as much as possible, was used as an electrolyte solution. The potential range of the CV test was set to 0.0-0.5 V (*vs* Ag/AgCl) with varying scan rates at 10, 50, 100, and 200 mV s^{-1}. The CV test was also carried out 10^4 times at 200 mV s^{-1} to examine the cycle performance of the Co-Ni oxide/Ni foam electrode. In addition, an impedance measurement was conducted after the CV test, using a frequency response analyzer (Autolab) in a constant voltage mode (0.00, 0.25, 0.50 V *vs* Ag/AgCl), by sweeping frequencies from 10^{-2} to 10^5 Hz at an amplitude of 5 mV.

Results and Discussion

Figure 1(a) shows the surface image of the pristine nickel foam, clearly revealing the three-dimensional network structure where active material may be included in both the surface pores and the inner cavities. The essential benefit expected by using the nickel foam as a current collector is the higher surface area by the surface pores and also possibly the higher packing density in the inner cavities, resulting in the improvement of electrode density. As shown in Figure 1(c), the Co-Ni mixed oxide electrode appears as a homogeneously coated phase on the surface of the nickel foam and as an effectively filled phase without any binder in the inner cavities. The bulk phase within the cavities of the nickel foam has many micropores that are generated during heat treatment, enabling the provision of a conducting route for the surface redox reaction inside the bulk material, thus promoting a capacitive property improvement. Another benefit obtainable here is that the redox reaction occurring on the surface of nickel foam itself can contribute to total capacitive properties, which is proved by the cyclic voltammogram of pristine nickel foam in Figure 1(b). The specific capacitance of the pristine nickel foam, estimated from the cyclic voltammogram, is about 45-70 F g^{-1}, which is nearly agreed with the previously reported values (50-65 F g^{-1}) for nickel oxides.[9,10]

The energy dispersive spectroscopy result in Figure 2(a) shows that the mixed oxide synthesized consists of cobalt and nickel species, confirming the elemental ratio of Co/Ni = 1:1, which is distributed on the electrode surface. The X-ray diffraction pattern in Figure 2(b) also shows that the crystalline phases can be proven to consist of NiO and Co_3O_4 crystalline phases. The peaks that appear near 2θ = 10 and 80° may be regarded as being due to the noise imparted by impurities, independent of the cobalt and nickel species.[26] The NiO phase can be confirmed by comparison with other results[11,27] and indicate that the peaks at 2θ = 37, 43, and 63° correspond to the (111), (200), and (220) planes of a NiO

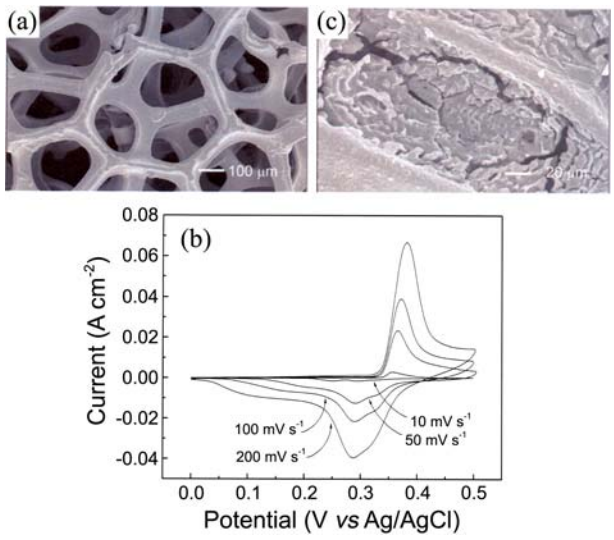

Figure 1. Surface images of (a) Ni foam and (c) Co-Ni oxide/Ni foam electrodes. The magnification ratios are (a) × 100 and (c) × 500. The cyclic voltammogram of pristine Ni foam is shown in (b).

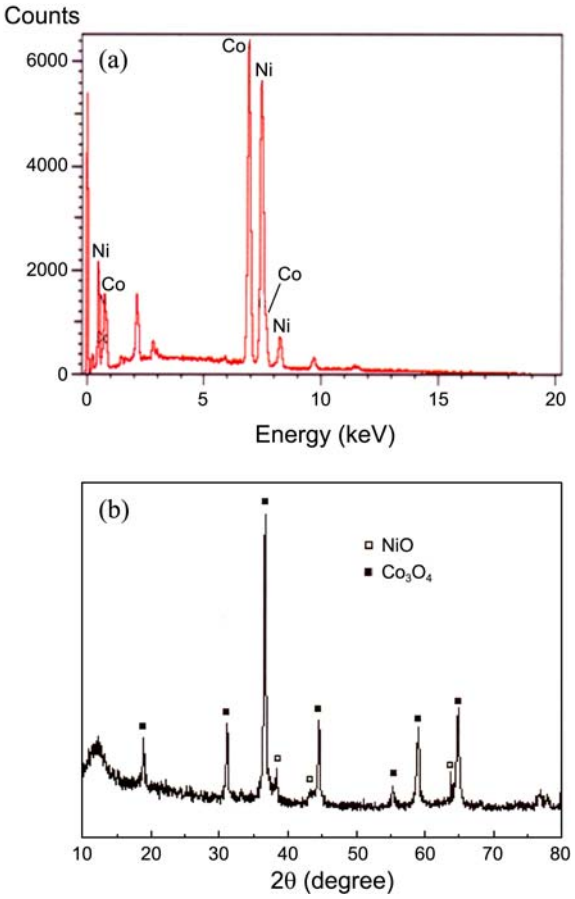

Figure 2. (a) Energy dispersive spectroscopy and (b) X-ray diffraction results of the synthesized Co-Ni oxide. Prior to X-ray diffraction, the Co-Ni oxide powder was directly sampled from the electrodes of Co-Ni oxide/Ni foam.

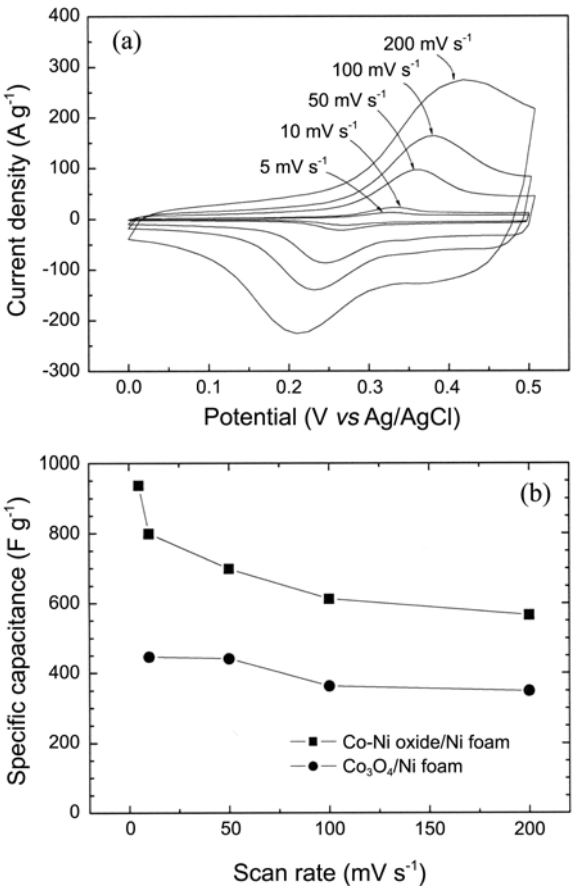

Figure 3. (a) Cyclic voltammogram of a Co-Ni oxide/Ni foam electrode at different scan rates and (b) the specific capacitance of Co-Ni oxide/Ni foam as a function of scan rate. The specific capacitance of the Co_3O_4/Ni foam electrode is also presented for comparison.

phase, respectively. The confirmation of Co_3O_4 phase can also be performed by comparison with other reports.[26,28] Considering that the crystalline phase of cobalt oxide may be changed by the annealing temperature, an amorphous structure of $Co(OH)_2$ may decompose to form CoO at temperatures over 160 °C, while the CoO transforms to the more oxidized form, Co_3O_4, by further increases in the annealing temperature.[9] The Co_3O_4 phase can be established because the annealing temperature is 250 °C in the present study. This agrees well with the fact that cobaltous oxide (CoO) is very reactive with oxygen and easily yields a high level of oxides, and that cobaltic oxide (Co_2O_3) exists normally as the hydroxide or transforms to a more stable phase, cobaltosic oxide (Co_3O_4), by absorbing oxygen at temperatures above 250 °C.[18]

Cyclic voltammograms for the Co-Ni oxide/Ni foam electrode are shown in Figure 3(a) as a function of scan rate. Comparing these with the shapes of some voltammograms from other reports,[21,26-28] the CV shapes at low scan rate (*e.g.*, 10-50 mV s^{-1}) are very close to that of a nickel oxide/carbon nanotube electrode[26] and a Co-Ni oxide/Ni mesh electrode,[27] in which the oxidation and reduction peaks appear at near 0.4 and 0.2 V, respectively. These redox peaks may correspond to the formation of nickel hydroxide at the surface of nickel oxide by the following reaction[29,30] in an aqueous KOH solution:

$$Ni(OH)_2 + OH^- \leftrightarrow NiOOH + H_2O + e^- \quad (1)$$

such that the redox transition of $Ni(OH)_2$/NiOOH can be suppressed by mixing the cobalt oxide[21] in the high potential range in which an oxygen evolution reaction may occur:[14,31]

$$Co_3O_4 + H_2O + OH^- \leftrightarrow 3CoOOH + e^- \quad (2)$$

$$CoOOH + OH^- \leftrightarrow CoO_2 + H_2O + e^- \quad (3)$$

As shown in Figure 3(a), the CV responses on the positive sweeps are symmetrical to their counterparts on the negative sweeps, which agrees well with previous reports for Co-Ni mixed oxide electrodes.[21,27] As well, larger oxidation and reduction peaks with the potential shifts in positive and negative directions, respectively, may originate from the nickel foam current collector itself (see Figure 1(b)), resulting in a similar CV pattern with increasing scan rate. Moreover, the effect of the nickel foam substrate may be enhanced at the higher scan rate because the redox reaction occurs more actively on the surface of nickel foam when charging and discharging at a high current rate.

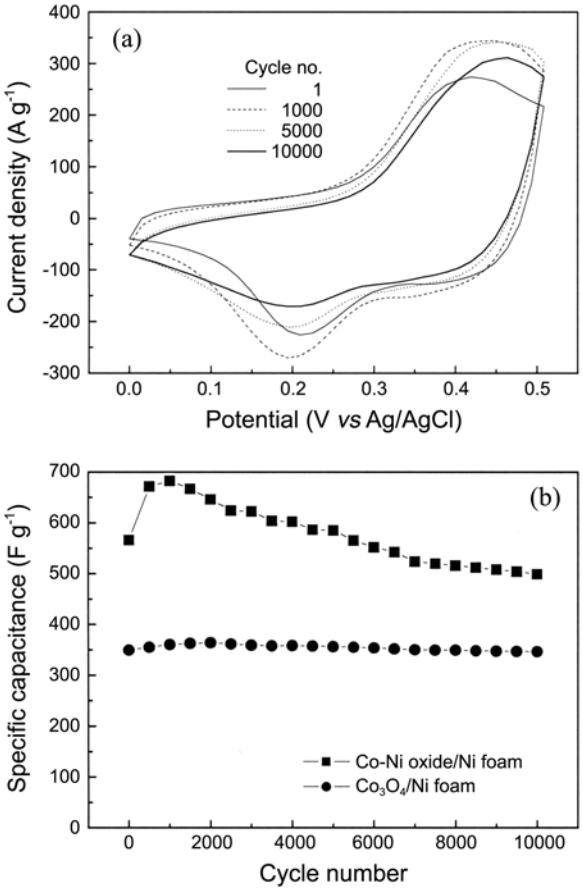

Figure 4. Cyclic voltammogram of a Co-Ni oxide/Ni foam electrode at 200 mV s^{-1} during cycle-life test and (b) the specific capacitance of Co-Ni oxide/Ni foam as a function of cycle number. The specific capacitance of Co_3O_4/Ni foam electrode was also presented for comparison.

Figure 3(b) shows the specific capacitance as a function of scan rate, which is calculated from the CV response as $C = (q_a + q_c)/2m\Delta V$, where C is the specific capacitance, q_a the anodic charge, q_c the cathodic charge, m the electrode mass, and ΔV the potential difference. As a result, the Co-Ni oxide/Ni foam electrode shows its highest capacitance, *e.g.*, 936 F g^{-1} at 5 mV s^{-1} and 556 F g^{-1} at 200 mV s^{-1}, compared to the previously reported capacitance values. He *et al.*[27] prepared an electrodeposited (Co+Ni)O_x (4:6) electrode on a nickel mesh and confirmed it to show 475 F g^{-1} at 20 mV s^{-1}. Fan *et al.*[26] also reported 569 F g^{-1} at 10 mA cm^{-2} using a composite electrode of Co-Ni oxide/carbon nanotube. The capacitance values (730 F g^{-1} at 25 mV s^{-1}) reported by Hu and Cheng,[21] using a Co-Ni oxide prepared by anodic deposition, can be compared with the results presented here. With a more rigorously consideration, however, it can be seen that this is a slightly different electrode material from our Co-Ni oxide/Ni foam because they used an amorphous Co-Ni hydroxide, (Co-Ni)$(OH)_2 \cdot nH_2O$, not the crystalline oxide. Thus, the present Co-Ni oxide/Ni foam electrode exhibits a superior capacitance value due to its excellent dimensional stability, which allows the Co-Ni oxide active material to persist and also provides supercapacitive properties sufficiently to the surface and even to the inside of the active bulk material.

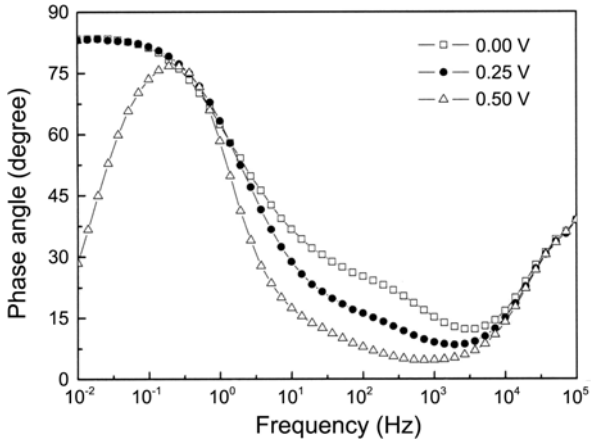

Figure 5. Frequency dependence of the phase angle in the impedance spectra of a Co-Ni oxide/Ni foam electrode. Electrolyte 1 M KOH (25 °C); amplitude 5 mV.

The cycle performance of the Co-Ni oxide/Ni foam electrode was also carried out by repeating the CV 10^4 times at 200 mV s^{-1} (see Figure 4). As the cycle number increases, the intensity changes (a decrease followed by an increase) in the oxidation and reduction peaks around 0.4 and 0.2 V, respectively, are clearly observed and reflect the saturation of specific capacitance followed by its initial increase and decrease, as shown in Figure 4(b). In particular, the reduction peak around 0.2 V, originating from the redox reaction occurring on the surface of the nickel foam,[32] can be explained as the nickel foam itself also contributing to the capacitive properties to a certain extent. Except for the cycle performance at the initial stages in the specific capacitance, the nearly saturated value of the Co-Ni oxide/Ni foam electrode reaches about 500 F g^{-1} after cycling 10^4 times operating at 200 mV s^{-1}. It can be expected that this is a much higher value than any other reports employing Co-Ni mixed oxides[21,26,27] and that of Co_3O_4/Ni foam electrode (about 350 F g^{-1}).[32]

On the other hand, the capacitor response frequency is analyzed from the impedance data (see Figure 5) in order to obtain information on the conduction mechanism of the Co-Ni oxide on the nickel foam substrate. According to Sugimoto *et al.*,[6] the low-frequency region is defined by the phase angle f as $-90^o < \phi < -45^o$ and the frequency where $\phi = -45^o$ can be recognized as the frequency response to the ideally capacitive behavior (capacitor response frequency $f_{\phi = -45}$). The $f_{\phi = -45}$ in the figure ranges from 1.6 to 4.2 Hz, giving the response time of the capacitor as 600-240 ms. This value is very similar to that of hydrous RuO_2 (500-250 ms) and layered RuO_2 hydrate (500-200 ms).[6] Comparing the response times, it can be assumed that the capacitor frequency response of the Co-Ni oxide/Ni foam electrode is dominated by the protonic and ionic conductions simultaneously. More precisely, it can be also expected by intuition that the protonic conduction mainly occurs on the surface, whereas the ionic conduction largely in the bulk through the

surface pores.

Conclusion

We prepared a Co-Ni mixed oxide, adopting the nickel foam as a current collector, to ensure the dimensional stability and to provide more probability of electrochemical active sites on the surface and the within the bulk electrode. As a result, we achieved a capacitance improvement of as much as 936 F g^{-1} at 5 mV s^{-1} and 566 F g^{-1} at 200 mV s^{-1}, and a comparatively good cycle performance with the Co-Ni oxide/Ni foam electrode. The conduction mechanism acting on this electrode was accomplished by both proton and ionic conductions, as determined from the analysis of capacitor response frequency.

Acknowledgments. This study was supported by a grant from the Fundamental R&D Program for Core Technology of Materials funded by the Ministry of Knowledge Economy of Korea. This study was also supported by the Converging Research Center Program through the Korean Ministry of Education, Science and Technology (2012K001259).

References

1. Lee, B. J.; Sivakkumar, S. R.; Ko, J. M.; Kim, J. H.; Jo, S. M.; Kim, D. Y. *J. Power Sources* **2007**, *168*, 546.
2. Song, R. Y.; Park, J. H.; Sivakkumar, S. R.; Kim, S. H.; Ko, J. M.; Park, D.-Y.; Jo, S. M.; Kim, D. Y. *J. Power Sources* **2007**, *166*, 29.
3. Ryu, K. S.; Jeong, S. K.; Joo, J.; Kim, K. M. *J. Phys. Chem. B* **2007**, *111*, 731.
4. Kim, I.-H.; Kim, J.-H.; Lee, Y.-H.; Kim, K.-B. *J. Electrochem. Soc.* **2005**, *152*, A2170.
5. Hu, C.-C.; Chang, K.-H.; Lin, M.-C.; Wu, Y.-T. *Nano Lett.* **2006**, *6*, 2690.
6. Sugimoto, W.; Iwata, H.; Yokoshima, K.; Murakami, Y.; Takasu, Y. *J. Phys. Chem. B* **2005**, *109*, 7330.
7. Chang, K.-H.; Hu, C.-C. *Appl. Phys. Lett.* **2006**, *88*, 193102.
8. Ke, Y.-F.; Tsai, D.-S.; Huang, Y.-S. *J. Mater. Chem.* **2005**, *15*, 2122.
9. Liu, K. C.; Anderson, M. A. *J. Electrochem. Soc.* **1996**, *143*, 124.
10. Srinivasan, V.; Weidner, J. W. *J. Electrochem. Soc.* **1997**, *144*, L210.
11. Nam, K.-W.; Kim, K.-B. *J. Electrochem. Soc.* **2002**, *149*, A346.
12. Lee, S.-H.; Tracy, C. E.; Pitts, J. R. *Electrochem. Solid-State Lett.* **2004**, *7*, A299.
13. Prasad, K. R.; Miura, N. *Appl. Phys. Lett.* **2004**, *85*, 4199.
14. Lin, C.; Ritter, J. A.; Popov, B. N. *J. Electrochem. Soc.* **1998**, *145*, 4097.
15. Liu, T.-C.; Pell, W. G.; Conway, B. E. *Electrochim. Acta* **1999**, *44*, 2829.
16. Srinivasan, V.; Weidner, J. W. *J. Power Sources* **2002**, *108*, 15.
17. Cao, L.; Lu, M.; Li, H.-L. *J. Electrochem. Soc.* **2005**, *152*, A871.
18. Shinde, V. R.; Mahadik, S. B.; Gujar, T. P., Lokhande, C. D. *Appl. Surf. Sci.* **2006**, *252*, 7487.
19. Kandalkar, S. G.; Gunjakar, J. L.; Lokhande, C. D. *Appl. Surf. Sci.* **2008**, *254*, 5540.
20. Hu, C. C.; Lee, Y. S.; Wen, T. C. *Mater. Chem. Phys.* **1997**, *48*, 246.
21. Hu, C. C.; Cheng, C. Y. *Electrochem. Solid-State Lett.* **2002**, *5*, A43.
22. Chen, J.; Bradhurst, D. H.; Dou, S. X.; Liu, H. K. *J. Electrochem. Soc.* **1999**, *146*, 3606.
23. Metzger, W.; Westfall, R.; Hermann, A.; Lyman, P. *Intern. J. Hydrogen Energy* **1998**, *23*, 1025.
24. Yan, D.; Cui, W. *J. Alloys Comp.* **1999**, *293-295*, 780.
25. Bispo-Fonseca, I.; Aggar, J.; Sarrazin, C.; Simon, P.; Fauvarque, J. F. *J. Power Sources* **1999**, *79*, 238.
26. Fan, Z.; Chen, J.; Cui, K.; Sun, F.; Xu, Y.; Kuang, Y. *Electrochim. Acta* **2007**, *52*, 2959.
27. He, K.-X.; Wu, Q.-F.; Zhang, X.; Wang, X.-L. *J. Electrochem. Soc.* **2006**, *153*, A1568.
28. Švegl, F.; Orel, B.; Hutchins, M. G.; Kalcher, K. *J. Electrochem. Soc.* **1996**, *143*, 1532.
29. Bouessay, I.; Rougier, A.; Tarascon, J.-M. *J. Electrochem. Soc.* **2004**, *151*, H145.
30. Nam, K.-W.; Lee, E.-S.; Kim, J.-H.; Lee, Y.-H.; Kim, K.-B. *J. Electrochem. Soc.* **2005**, *152*, A2123.
31. Wen, T.-C.; Hu, C.-C.; Lee, Y.-J. *J. Electrochem. Soc.* **1993**, *140*, 2554.
32. Yoon, Y. I.; Kim, K. M.; Ko, J. M. *J. Korean Ceram. Soc.* **2008**, *45*, 368.